Fluorescence Emission Spectral Shift Measurements of Membrane Potential in Single Cells

W. Y. Kao,* C. E. Davis,† Y. I. Kim,*§ and J. M. Beach*
*Departments of *Biomedical Engineering and §Neurology, University of Virginia Health Sciences Center, Charlottesville, Virginia 22906 USA, and †Department of Physiology, Johns Hopkins University, Baltimore, Maryland 21205 USA

ABSTRACT Previous measurements of transmembrane potential using the electrochromic probe di-8-ANEPPS have used the excitation spectral shift response by alternating excitation between two wavelengths centered at voltage-sensitive portions of the excitation spectrum and recording at a single wavelength near the peak of the emission spectrum. Recently, the emission spectral shift associated with the change in transmembrane potential has been used for continuous membrane potential monitoring. To characterize this form of the electrochromic response from di-8-ANEPPS, we have obtained fluorescence signals from single cells in response to step changes in transmembrane potentials set with a patch electrode, using single wavelength excitation near the peak of the dye absorption spectrum. Fluorescence changes at two wavelengths near voltage-sensitive portions of the emission spectrum and shifts in the complete emission spectrum were determined for emission from plasma membrane and internal membrane. We found that the fluorescence ratio from either dual-wavelength recordings, or from opposite sides of the emission spectrum, varied linearly with the amplitude of the transmembrane potential step between −80 and +60 mV. Voltage dependence of difference spectra exhibit a crossover point near the peak of the emission spectra with approximately equal gain and loss of fluorescence intensity on each side of the spectrum and equal response amplitude for depolarization and hyperpolarization. These results are consistent with an electrochromic mechanism of action and demonstrate how the emission spectral shift response can be used to measure the transmembrane potential in single cells.

INTRODUCTION

Optical techniques using potentiometric probes have been successfully used to monitor electrical phenomena in cells and tissue where microelectrode access is not possible. Studies with imaging and multi-site recording methods have characterized spread of cardiac potentials (Salama et al., 1987; Efimov et al., 1994), neuronal activity in cerebral cortex (Orbach et al., 1985; London et al., 1989), and more recently impulse propagation in heart cells (Rohr and Salzberg, 1994). Most of these techniques used single-wavelength recording, and calibration depended on external factors such as the degree and distribution of dye label. In addition, voltage responses varied widely in different cell systems because voltage-sensing mechanisms involved interaction of the membrane electric field with molecular orientation, or depended on fluorescence-quenching after voltage-dependant aggregation of the probe (Loew et al., 1985).

To obtain more uniform response in various cell types, Loew and associates developed membrane probes based on aminostyrylpyridinium (ASP) chromophores that exhibit electrochromic responses wherein the field interacts directly with electronic states (Loew et al., 1979; Loew and Simpson, 1981). These membrane-bound ASP probes were shown to exhibit electrochromism resulting from a charge-shift mechanism in which energies of absorption, excitation, and emission are modulated by the membrane electric field strength (Loew et al., 1985). Fluorescence spectral shifts were associated with voltage response and were shown to be of similar magnitude in excitation and emission spectra from hemispherical bilayers labeled with di-4-ANEPPS, a naphthyl analog of the ASP probe (Fluhler et al., 1985). This strong electrochromic response from di-4-ANEPPS was confirmed in lipid bilayers (Montana et al., 1989) and later in several cell systems (Gross et al., 1986; Ehrenberg et al., 1987; Montana et al. 1989). A ratiometric dual-excitation method demonstrated the linearity of voltage response and repeatability in specific cell types (Montana et al., 1989). The sensitivity and reproducibility of the ratio method yielded a measurement precision of 10 mV, enabling studies of electrical responses in nonexcitable cells and tissue. The probe di-8-ANEPPS was introduced with a longer chain-length (Ehrenberg et al., 1990) to improve membrane stability; most subsequent work used this new probe. Numerous applications of styryl voltage probes in model membranes, cells, and tissues were documented in a review of potentiometric dye studies (Loew et al., 1992). Nonelectrochromic responses of these probes were also present in different cell systems to various degrees (Loew et al., 1985, 1992). The linearity of voltage-induced fluorescence excitation ratios from di-8-ANEPPS was further tested and confirmed by manipulating potential in single cells using patch-clamp and imaging cell fluorescence (Zhang et al., 1998). The linear response of both di-4- and di-8-ANEPPS has also been exploited without ratio recording in excitable cells, using only changes in red fluorescence

Received for publication 16 April 1999 and in final form 3 May 2001.

Address reprint requests to J. Beach, Cellomics, Inc., 635 William Pitt Way, Pittsburgh, PA 15101. Tel.: 412-826-3600, ext. 2906; Fax: 412-826-3850; E-mail: jbeach@cellomics.com.

0006-3495/01/08/1163/08 $2.00

to monitor membrane potential behavior in cardiac cells and tissue during field stimulation (Knisley et al., 1999; Cheng et al., 1999). In these studies of the coupling relationship between cell response and field stimulation parameters, and of the role of fiber structure on cardiac stimulation, the linearity of the dye response was confirmed over a wide range of membrane potential by simultaneous recordings of the action potential (Cheng et al., 1999).

Recently a single-wavelength excitation method using emission spectral shifts for ratio monitoring of the membrane potential was developed using di-8-ANEPPS (Beach et al., 1996). In this technique, fluorescence was monitored simultaneously at two voltage-sensitive wavelengths located on the wings of the emission spectrum. Use of simultaneous wavelength monitoring provides an advantage over alternating excitation in mechanical simplicity. More importantly, lower measurement noise and improved accuracy can be achieved because variations in excitation strength are canceled during each recording point, and there is complete temporal overlap of both fluorescence signals with the period of voltage change. This emission-shift method was developed to record microvascular membrane potential changes from nonexcitable cells, which are typically <50 mV. Ability of the ratiometric emission signal to follow membrane potential during tissue motion accompanying vasomotor response was demonstrated and voltage sensitivity was established by co-recordings with a microelectrode. The method was used to measure relatively small and slow (<11 mV, >1 S) membrane potential signals in vascular endothelium associated with electrotonic spread of current along microvessels during conducted vasomotor activity (Beach et al., 1998) and produced the first recordings of membrane potential changes from capillaries (McGahren et al., 1998).

In excitable cells, di-8-ANEPPS dual-emission recordings were first characterized in cultured neurons undergoing fast membrane potential steps (50-ms pulse) by patch clamp (Bullen and Saggau, 1999). Their results showed that photobleaching occurred equally at both recorded wavelengths from each side of the emission spectrum over the course of short periods up to 600 ms. Although the absolute ratio of fluorescence emission varied linearly with potential, and the slope was approximately constant in all cells, their results showed an uncertainty of $\sim$10% in the value of the ratio at any given membrane potential among cells and across recording sites of the same cell. This variable offset in the ratio was larger than voltage-dependent ratio changes between -120 and 60 mV. They obtained relatively consistent responses by normalizing recorded ratios by the value obtained when membrane potential was brought to zero using K^+-selective ionophores. Recording this normalizing parameter at each recording site enabled comparison of voltage changes with an accuracy of 5 mV. These results of Bullen and Saggau (1999) and of Zhang et al. (1998) together demonstrate that rapid membrane potential recording with linear response can be obtained by analysis of fluorescence changes arising from voltage-induced shifts of either the dye excitation or the emission spectrum.

Ratiometric measurement technique is potentially useful as a continuous monitor for membrane potential in nonexcitable cells and tissues over longer time periods. In this report, we characterize the emission spectral shift response of di-8-ANEPPS in nonexcitable human embryonic kidney (HEK 293) cells using dual-wavelength and complete spectral recording techniques together with cell patch clamp control of the transmembrane potential. HEK 293 cells were chosen because the spherical whole-cell configuration is mechanically stable and easy to frame within a square photometer window. We evaluate the stability of the time and voltage dependence of dual-wavelength recordings at 560 nm and 620 nm over periods of up to 60 s under continuous excitation. Dye emission spectral changes, obtained by imaging the spectrum of fluorescence from single cells, are also presented for comparison with excitation difference spectra previously published by Montana et al. (1989), along with a description of the prism spectrographic camera used for these measurements. Relative changes in the emission spectral amplitude resulting from excitation spectral shifts or effects other than electrochromism on dye response are not addressed in this study.

MATERIALS AND METHODS

Culture of HEK 293 cells

Human embryonic kidney (HEK 293) cells (American Type Culture Collection, Rockville, MD) were cultured at 37°C in Dulbecco's modified essential medium (DMEM, Life Technologies, Grand Island, NY) supplemented with 10% FBS and 1% penicillin-streptomycin. Cells were plated onto poly-L-lysine-coated glass coverslips (1-inch diameter) and incubated in fresh media for one hour before use. After cells became immobile, media were replaced with DMEM containing 6 μM di-8-ANEPPS and 0.1% Pluronic detergent. Cells were stained for 20 min at 37°C and rinsed once before replacing fluid with 2 ml of solution containing (in mM): 130 NaCl, 5 KCl, 10 $CaCl_2$, 5 glucose, and 10 HEPES (pH 7.2).

Whole cell voltage patch-clamp

Patch-clamp was applied to cells using standard techniques (Hamill et al., 1981). Briefly, patch electrodes of Kimax capillary tubing (1.5–1.8 mm outer diameter; American Scientific Products, Golden, CA) were pulled on a two-stage List L/M-3P-A patch pipette puller (List Electronics, Darmstadt, Germany). The glass electrode tips were then heat-polished using a List L/M-CPZ-101 pipette forge to a final 1–2 Mohm resistance. The internal pipette solution contained (in mM) 1 $CaCl_2$, 2 $MgCl_2$, 120 CsCl, 11 EGTA, 20 TEA-Cl and 10 HEPES (pH 7.2). Once whole-cell configuration was achieved, cells were voltage-clamped using pClamp 5.5.1 software (Axon Instruments, Foster City, CA) with a List EPC-7 amplifier. For dual-wavelength experiments, two voltage protocols were used: 1) 16 pulses between -80 mV (hold potential) and $+60$ mV (test potential) with 2.5-s pulse duration, 50% duty cycle (STEP protocol); and 2) 16 pulses from -80 mV holding potential to test levels starting at -60 mV and incrementing 10 mV/pulse to $+90$ mV, 2.5-s pulse duration, 50% duty cycle (RAMP protocol). For spectral imaging experiments, the command

sequence was: negative test potential, 0 mV, negative test potential, positive test potential; 5-s potential duration, while the camera shutter was actuated to expose during pulses.

Fluorescence recordings

Cells were viewed and imaged through an inverted microscope (Zeiss Axiovert 100, 90X oil immersion; Carl Zeiss, Inc., Thornwood, NY). Excitation light was obtained from a model 1010 150 W stabilized xenon arc source (PTI Inc., South Brunswick, NJ) with a single monochromator illuminator (L1/FM-100). The excitation wavelength (480 nm) was chosen by sweeping the monochromator passband (20 nm width) to obtain the brightest dye emission from labeled cells. Illumination was reduced with a 1-OD neutral density filter to avoid excessive bleaching and phototoxic effects. Light was directed to the microscope stage with a dichroic beam splitter (FITC) and fluorescence was collected through a 510-nm barrier filter. Dual-wavelength signals were recorded with a PTI model D104 microscope photometer containing a second dichroic splitter with bandpass filters (560- and 620-nm, 20 nm passbands) in the path to each PMT. Recording wavelengths were chosen to match voltage-sensitive portions of the emission spectrum (Beach et al., 1996). The recording aperture left a margin around the cell of one-quarter of the cell diameter, which included the tip of the patch pipette. PMT voltages were adjusted to give at least 5×10^5 counts/s on each channel, with the gain of one channel adjusted to achieve an initial ratio equal to one before recording (Gross et al., 1994). Initialization of the ratio to one was done to facilitate comparison of ratio changes, and was shown by Gross et al. to maximize the linearity of the dye response in their dual-excitation method. Data were acquired at 100 Hz using PTI fluorescence software (OSCAR).

Spectral images were obtained with increased excitation intensity (0.5-OD filter in path) to compensate for decreased sensitivity of the CCD camera relative to PMTs. A prism-type spectrograph (400–700 nm range; Edmund Scientific, Barrington, NJ) was placed in the path of the emerging beam, held centered in a sleeve-type coupling mechanism which was attached to the faceplate of a chilled CCD camera (512 × 512 pixel 18-bit grayscale; EG&G OMA). Pixel columns were aligned parallel with the spectrograph slit. Prism optics were chosen because the single refracted light spectrum provided greater light throughput than could be achieved with a grating-type spectrograph with similar spectral resolution. The microscope stage was translated under transillumination to position the center of the cell in the spectrograph entrance slit before attaching the clamp electrode. Focus at the spectral camera was then determined under epiillumination. Spectral images were acquired using 2-s light integration periods which began and ended during clamp episodes of holding and command voltages. Wavelengths were calibrated before each experiment by recording transillumination through a series of narrow bandpass filters which overlap the dye emission spectrum (558-, 586-, 605-, 650-nm) and determining the pixel location at the center of each band. The relationship between pixels along rows of the image and wavelength was found by performing third order polynomial regression between the recorded positions and the wavelengths of filter spectral peaks. Dye spectra were plotted with the *x* axis containing actual wavelengths instead of the pixel positions, resulting in a linear wavelength axis. Filter spectral peaks were determined near both upper and lower edges of the spatial axis to check for rotation between the spatial and wavelength axes. The variation of the microscope light collection optics, spectrograph and camera responses with wavelength were corrected by assuming the approximation of constant radiance from the xenon source between 500 and 700 nm, and recording the xenon emission spectrum from light reflected into the objective lens. Dye spectral intensities were then corrected by normalization with this spectrum. The exact radiance versus wavelength of the source is not known. However, typical radiance versus wavelength profiles show that the source intensity increases gradually with wavelength. This effect would slightly blue-shift our corrected spectra; however, it would not affect analysis of spectral shifts obtained from area-normalized spectra.

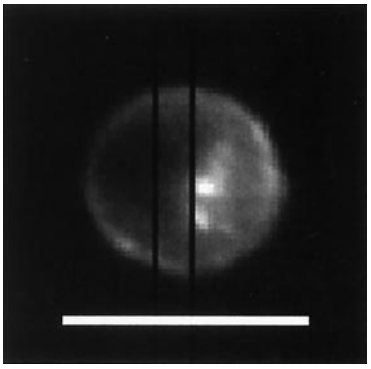

FIGURE 1 Labeled HEK cell viewed under epiillumination. Cell shows diffuse membrane fluorescence with moderately bright localized intracellular emission. Typical slit location marked by rectangle in *black*. Horizontal bar, 10 μm.

Data analysis

Fluorescence ratios from dual-wavelength continuous recordings were obtained by dividing the data values at each wavelength using a spreadsheet program (Origin, Microcal software, Northampton, MA). Spectral curves were obtained from images by scanning a 10-pixel wide band of pixels horizontally across the image outside the cell spectrum at least 20 pixels from the edge of the spectrum, and within the cell spectrum near the edges and center of the spectrum, using a custom program. Baseline-corrected spectra were obtained by subtracting dark scans from intracellular scans. Areas under spectral curves were first normalized to the same value before curves were subtracted. Wavelength axes were always determined from filter calibrations taken before recordings on the same day.

RESULTS

Dye label

Cells viewed under epiillumination showed brighter emission near the edge of the cell corresponding to dye in the outer plasma membrane. Typically, the cell interior was less fluorescent just within the outer edge and showed variable degrees of brighter intensity near the cell center which appeared either diffuse or localized (Fig. 1). The source of this fluorescence is believed to be dye internalized into intracellular membrane. The degree of intracellular emission increased over time after cells were switched back to solutions that did not contain dye. The final degree of dye-internalization was not affected by extending the time of loading past that required to obtain plasma membrane fluorescence. Background fluorescence surrounding cells was negligible.

Dual-wavelength recordings

Fluorescence traces recorded during repeating step protocols showed opposing changes in intensity at the two wavelengths which coincided with edges of each 140-mV command pulse. Fig. 2 (*top*) shows traces recorded from a cell in which intracellular fluorescence was not yet present in

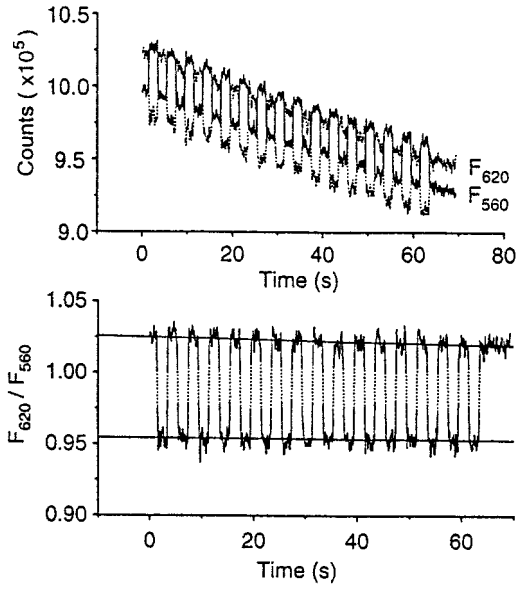

FIGURE 2 Results from dual-wavelength recording with STEP voltage control. (*Top*) Fluorescence traces (*solid line*, 560 nm; *dotted line*, 620 nm) during 16 pulses from −80 mV (beginning and end of traces) to +60 mV (ΔV = 140 mV). (*Bottom*) Fluorescence ratio F_{620}/F_{560}, corresponding to a ratio change of 0.051/100 mV. Bold portions of the records mark periods of holding and test voltage periods parsed from the direct ratio trace. *Solid lines* are best fits to parsed data.

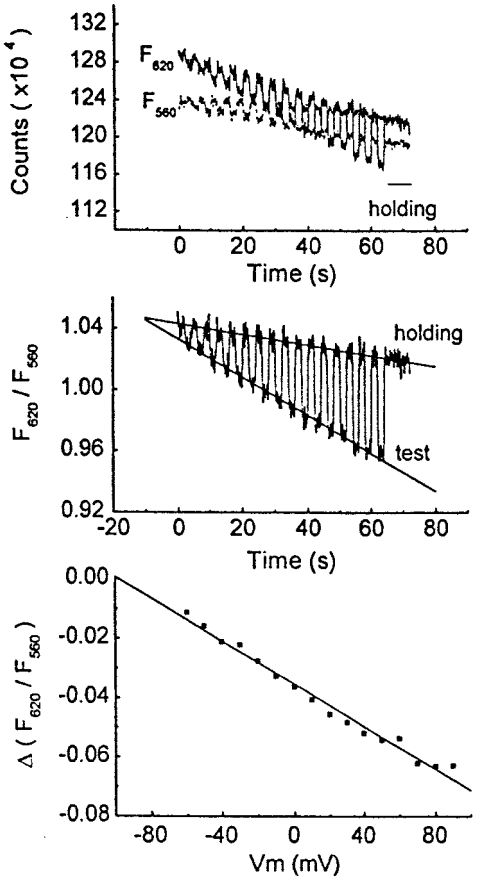

FIGURE 3 Results from dual-wavelength recording with RAMP voltage control. (*Top*) Fluorescence traces (*dotted line*, 560 nm; *solid line*, 620 nm) during 16 command pulses from −80 mV to between −60 mV and +90 mV in 10 mV-amplitude increments. (*Center*) Parsed fluorescence ratio with best fitting lines. (*Bottom*) Amplitudes of F_{620}/F_{560} ratio steps at each voltage change plotted against size of voltage change. Slope of best fitting line is −0.034/100 mV.

noticeable amounts. Intensity of fluorescence at both wavelengths decays by 5% in approximately 50 s (0.1%/s). Although this is a relatively modest rate of bleaching, it should be noted that slow membrane potential changes could be masked if fluorescence signals at either wavelength were used as the voltage indicator. The fluorescence ratio F_{620}/F_{560}, plotted in Fig. 2 (*bottom*), contains pulses of uniform amplitude over the series of command voltage periods. In this case where decay was similar for both fluorescence signals, the ratio alternated between two fixed values during the recording and was not sensitive to the time-dependence of the raw signals. This cell yielded a voltage sensitivity of 5.1% change in ratio per 100 mV. The average sensitivity from five cells, including the cell of Fig. 2 and four cells showing degrees of internal fluorescence, was 4.0 ± 0.75 SE %. Among all sampled cells, slow time-dependent decreases in intensity between 0.5% and 5% per minute were observed and were not necessarily equal at both wavelengths. Although these rates are low compared with many bleaching rates encountered using fluorescence probes, the effect of this magnitude of decay over time is comparable to the voltage response of the dye and could thus interfere with slow membrane potential recordings. However, if decay is similar at both wavelengths, the ratio signal responds specifically to the membrane potential changes.

Ramp protocols using 10-mV step increments from −60 mV to +90 mV also resulted in opposing intensity changes at each wavelength with a slow time-dependent component. The pair of signals recorded in one cell (Fig. 3, top panel) shows an approximately fourfold difference in the rate of signal attenuation at the two wavelengths, the largest disparity in slopes encountered in our measurements. This cell showed moderately bright localized emission near the center. Fluorescence recorded from this region of the cell probably included emission from dye in plasma and internal cell membranes. In this case, where decay rates differed significantly, the ratio values obtained during holding potentials showed a discernible slope = −2.4%/min (Fig. 3, *center*) and, therefore, slow membrane potential changes could be masked in the ratio signal if the voltage-independent trend is not known. Fractional changes in fluorescence ($\Delta F/F$) were proportional to the size of the potential step at both wavelengths, whereas the ratio of fractional changes, $(\Delta F/F)_{620}/(\Delta F/F)_{560}$, was nearly independent of the size of the potential change (Table 1). The difference between ratio

TABLE 1 Fractional changes in fluorescence

	80-mV step (%)	150-mV step (%)
% $\Delta F/F$ (620 nm)	1.20	2.12
% $\Delta F/F$ (560 nm)	2.21	4.13
$(\Delta F/F)_{620}/(\Delta F/F)_{560}$	0.54	0.51

values, $\Delta(F_{620}/F_{560})$, of adjacent holding and test potentials (averaged over the 80% of the pulse duration away from transitions), varied linearly with the size of the potential step (Fig. 3, *bottom*). A least-squares line fit through these points yielded a value for R (goodness-of-fit) of -0.9915 over the full range in test potentials. The average slope of this line for five cells (scale factor between ratio change and voltage) was $-3.6 \pm 0.1\%$ per 100 mV. These results demonstrate the linear response of the di-8-ANEPPS ratio signal from dual-emission recordings and show potential for interference from internal dye fluorescence.

Spectral imaging

Fig. 4 contains spectral images from four cells with increasing degrees (*top* to *bottom*) of internal fluorescence. Images show the spatial distribution of fluorescence from the cell structure across the vertical dimension, with the wavelength range across the horizontal dimension. Intensity near upper and lower boundaries of spectra presumably come from dye in the plasma membrane. Bright horizontal bands between upper and lower edges arise from dye internalized within the cell. Corrected spectral curves from a single cell that showed bright internal fluorescence are shown in Fig. 5. The pair of curves at right (*solid* and *dashed lines* with crossover wavelength near 600 nm) are spectra-obtained at -80 mV (*solid*) and $+80$ mV (*dashed*) by scanning horizontally near the edge of the spectral image. The $+80$ mV membrane spectrum is blue-shifted relative to that of the -80 mV membrane spectrum. The pair of curves to the left are spectra scanned through the area of bright internal fluorescence from the spectral image at the same potentials (-80 mV: *solid*; $+80$ mV: *dashed*). These spectra associated with internal fluorescence fall at shorter wavelengths and exhibit a smaller voltage-dependent spectral shift than those obtained near the cell edge. All spectra show asymmetric Gaussian shapes similar to those of previously published di-8-ANEPPS emission spectra (Loew et al., 1992). This asymmetry in the emission spectrum is opposite that of dye excitation spectra, with the steepest slope on the short wavelength side. In HEK cell plasma membranes, the spectral peak was near 605 nm and the half-width was 90 nm.

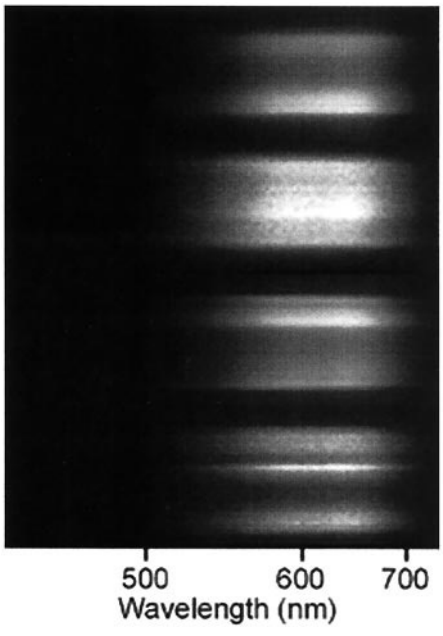

FIGURE 4 Dye fluorescence emission spectral images from different cells recorded with a prism-spectrographic camera. Patch electrode was attached to cell away from area under recording slit. Focus is set to obtain maximally sharp spectral edge. Cell spectra show membrane label at upper and lower edges with increasing degrees of diffuse and localized intracellular label (*top* to *bottom*). Images also show areas of slightly decreased intensity near central spectral wavelengths which were caused by nonuniform transmission versus wavelength in the excitation dichroic mirror. This artifact is commonly seen near the transition wavelength in the passband of dichroic mirrors and was removed as described in Methods. Horizontal axis: wavelength (460–700 nm) with cell fluorescence visible between 510 nm and 700 nm. Wavelength scale of the prism refraction spectrum is progressively compressed at longer wavelengths. Vertical axis: spatial dimension along slit, resolution <1 μm.

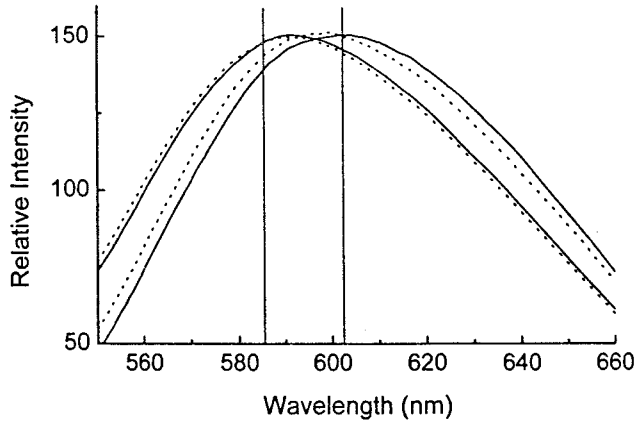

FIGURE 5 Corrected dye emission spectral curves from di-8-ANEPPS in a cell which showed marked internal dye fluorescence similar to that of the cell in Fig. 1. Cell regions containing the edge of the cell and the bright area of internal fluorescence were positioned within the spectrograph slit. Spectral curves were obtained by scanning horizontally across recorded spectral images. All spectra were normalized to the same area under the curve. (*Solid lines*) -80 mV. (*Dotted lines*) $+80$ mV. The spectral pair with crossover wavelength near 600 nm (at *right*) was scanned from the edge of the spectral image (containing mostly plasma membrane dye). The second pair with crossover wavelength near 585 nm was scanned through the region of the spectral image formed from internal fluorescence. A F_{620}/F_{560} ratio change of 6.5%/100 mV corresponds to the spectral shift from the first spectral pair.

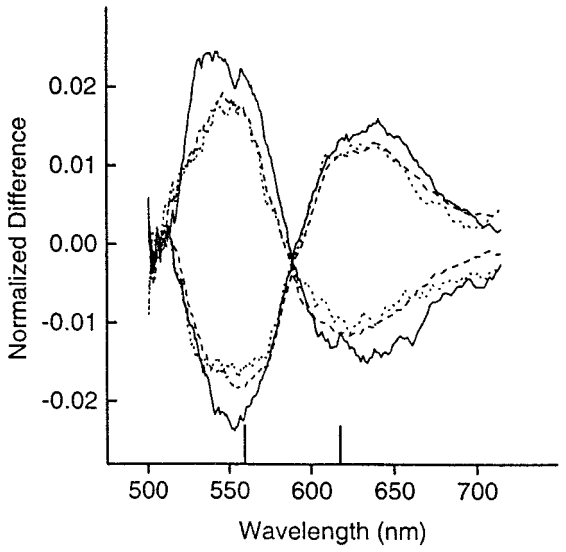

FIGURE 6 Difference spectra obtained from subtracting corrected dye emission spectra after adjusting areas under all spectra to that under the −80 mV edge (membrane) spectrum. Cell contained a moderate level of intracellular dye emission, and produced a spectrum similar to the upper middle spectrum of Fig. 4. Six spectra are included. The three difference curves with negative peaks near 550 nm and positive peaks near 630 nm resulted from subtracting +80 mV spectra from 0 mV spectra. Subtracting −80 mV spectra from 0 mV spectra produced the three curves of opposite polarity. Spectra cross at a single wavelength near the emission peak. Crossover varied by ±5 nm across all cells. (*Solid lines*) Scanned near edge of cell spectral image containing mostly plasma membrane emission. (*Dotted lines*) Scanned from center of cell spectral image containing emission from internalized dye and plasma membrane. (*Dashed lines*) Scanned from entire cell spectral image.

Fig. 6 shows difference spectra obtained with voltage steps to 0 mV and +80 mV from a holding potential of −80 mV. These spectra are scanned from a spectral image in which sites of intracellular fluorescence were not discernible (as in top spectrum of Fig. 4). Curves found by subtracting the spectrum at −80 mV from the spectrum at 0 mV show a short wavelength maximum and a long wavelength minimum. Curves found by subtracting the spectrum at −80 mV from that at 0 mV are of opposite polarity but otherwise show similar shapes and amplitudes. This second difference did not come from a single step change in potential but rather by comparison of spectra obtained from separate portions of the protocol. The largest amplitude (*solid line*), scanned horizontally near the top edge of the image, corresponds primarily to plasma membrane emission at the cell edge. Dotted and dashed lines, which were scanned horizontally across the full image (*dotted*), and the central portion of the image (*dashed*), show reduced spectral amplitudes, suggesting presence of internal dye that is not yet concentrated at interior sites. Peak wavelengths are close, but not identical, to wavelengths of maximal voltage sensitivity (*vertical lines*) found previously for endothelial cells (Beach et al., 1996). These difference spectra show that polarization of the membrane in each direction gives similar spectral shapes of opposing sign. These spectra mirror the shape of excitation difference spectra previously published from vesicles (Montana et al., 1989), with the higher peak amplitude at shorter wavelength. Areas averaged under positive and negative bands of the emission difference spectrum were nearly equal (1.142 vs. −1.141, edge and center spectra included in average), suggesting that a simple spectral shift accompanies the change in membrane potential.

DISCUSSION

We have applied multiwavelength fluorescence recording with voltage control by whole-cell patch clamping to measure changes in membrane potential from spectral emission shifts in single nonexcitable cells. Dual-wavelength recording at voltage-sensitive wavelengths of 560 nm and 620 nm showed opposing changes in intensity during steps in voltage, and produced a fluorescence ratio which varied linearly with the size of the step over a wide range of potentials extending both sides of 0 mV. These outcomes suggest that signals arose from wavelength shifts in the emission spectrum which are proportional to transmembrane potential changes, and that the emission shift remains linear with membrane potential, similarly to the excitation ratio (Montana et al., 1989). Further confirmation of a spectral shift origin for the signal comes from the fact that emission difference spectra from before and after voltage changes were mirror images of those previously reported from excitation spectra, with crossover wavelengths at or near the emission peak. The fact that crossovers remained constant for a given cell irrespective of whether the recorded spectral image was scanned only at the edge, corresponding to the cell edge, or included central regions, suggests that no internal dye responded to voltage changes.

Although dye emission spectra were not symmetric, the nearly equal areas under positive and negative bands in difference spectra indicate equal change in emission intensity on both sides of the spectrum, consistent with an electrochromic voltage response. The size of ratio changes obtained from HEK cells by the dual-emission technique was smaller by a factor of two than other values which have been obtained in single cells by dual-excitation recording (Montana et. al., 1989, Loew et al., 1992, Zhang et al., 1998) and in vascular cells by dual-emission recording (Beach et al., 1996). This may imply that additional nonelectrochromic effects were also present. However, voltage responses are known to vary between cell types of different membrane structure (Loew et al., 1992), and the ratio values also depend on instrumental factors. A means of standardizing values from different recorders could facilitate comparison of ratio results obtained on different equipment (Beach and Duling, 1993; Beach, 1997). In our experiments, photobleaching and wide-band excitation used to obtain the

spectra precluded an evaluation of nonelectrochromic voltage responses.

Analysis of dye emission spectra showed that the magnitude of the emission shift was equal but of opposite polarity for positive and negative steps in membrane potential. This behavior is consistent with the single slope in ratio response obtained by dual emission technique from −80 to +60 mV. Therefore, analysis of recorded spectral images from di-8-ANEPPS appears to provide a second means of monitoring change in membrane potential, and in addition, permits imaging of spectral changes along one dimension, and verification that signals arise from spectral shifts. Regarding this second advantage, we were previously able to show with spectral imaging that, in blood-filled microvessels, spectral shifts are detected without interference at the edge of the vessel, whereas further toward the center of the vessel reabsorption of fluorescence by the blood interfered with detection (Beach et al., 1996). This ability to confirm the shift in spectrum will also be important when membrane potentials must be followed by microscopy in cells or tissue undergoing motion. Causes of artifacts generated in dual-wavelength ratio recording include motion from the plane of focus without perfect chromatic correction and motion across the recording field when recorded areas do not perfectly overlap.

Our results showed that over many seconds different photodecay rates can be observed for red and green channels. This might be explained by an apparent spectral shift during dye internalization. If emission from dye in plasma and internal membranes have separate spectra as in Fig. 5, the total emission will shift toward blue wavelengths over time if signals include emission from areas central to the cell. In the absence of photobleaching, the red signal would decrease whereas the green signal increased. If photobleaching occurred over this time interval, red signals would decay faster than green signals. Our spectral and dual-wavelength data are consistent with this scheme. These results suggest that, to monitor slow membrane potential signals or resting potentials from single cells, fluorescence from regions with internal dye emission should be avoided either by use of a suitable aperture or by imaging the fluorescence. This interference from internalized dye could have contributed to site-dependent offsets in voltage sensitivity reported previously in neurons (Bullen and Saggau, 1999), and could also be present using dual-excitation technique if excitation spectra were different for plasma membrane and internal locations.

The dual emission method appears to provide for continuous recordings of membrane potentials, both on fast subsecond time scales as shown by Bullen and Saggau (1999), and over tens of seconds in recordings from nonexcitable cells. Spectral imaging will allow comparison of membrane potentials at different sites, and should continue to be useful for evaluation of electrochromic response in different cell membranes. This technique can also be useful for simultaneous recordings of membrane potential and motion associated with coupled motor responses. Future work will combine advantages of spatial mapping by imaging with multiple-emission wavelength recording.

This study was supported by grant HL-49593 and NS-38159 from the National Institutes of Health, and a research grant from the Muscular Dystrophy Association. It was presented in part at the Biophysical Society meeting in 1997. W.Y.K. and C.E.D. contributed equally to this study and are considered co-first authors.

REFERENCES

Beach, J. M. 1997. A LED light calibration source for dual-wavelength microscopy. *Cell Calcium.* 21:63–68.

Beach, J. M., and B. R. Duling. 1993. A light-emitting diode light source for photo-and videomicroscopy. *J. Microscopy.* 172:41–48.

Beach, J. M., E. D. McGahren, and B. R. Duling. 1998. Electrical communication exists between arterioles and capillaries in the hamster cheek pouch. *Am. J. Physiol.* 275:H1489–H1496.

Beach, J. M., E. D. McGahren, J. Xia, and B. R. Duling. 1996. Ratiometric measurement of endothelial depolarization in arterioles with a potential-sensitive dye. *Am. J. Physiol.* 270:H2216–H2227.

Bullen, A., and P. Saggau. 1999. High-speed, random access fluorescence microscopy. II. Fast quantitative measurements with voltage-sensitive dyes. *Biophys. J.* 76:2272–2287.

Cheng, D. K., L. Tung, and E. A. Sobie. 1999. Nonuniform responses of transmembrane potential during electric field stimulation of single cardiac cells. *Am J. Physiol.* 277:H351—H362.

Efimov, I. R., D. T. Huang, J. M. Rendt, and G. Salama. 1994. Optical mapping of repolarization and refractoriness from intact hearts. *Circulation.* 90:1469–1480.

Fluhler, E., V. G. Burnham, and L. M. Loew. 1985. Spectra, membrane binding, and potentiometric responses of new charge shift probes. *Biochemistry.* 24:5749–5755.

Gross, D., L. M. Loew, and W. W. Webb. 1986. Optical imaging of cell membrane potential changes induced by applied electric fields. *Biophys. J.* 50:339–348.

Gross, E., R. S. Bedlack, Jr., and L. M. Loew. 1994. Dual-wavelength ratiometric fluorescence measurement of the membrane dipole potential. *Biophys. J.* 67:208–216.

Hamill, O. P., A. Marty, E. Neher, B. Sakmann, and F. J. Sigworth. 1981. Improved patch-clamp techniques for high-resolution current recording from cells and cell-free membrane patches. *Pflugers Arch.* 391:85–100.

Knisley, S. B., N. Trayanova, and F. Aguel. 1999. Roles of electric field and fiber structure in cardiac electric stimulation. *Biophys. J.* 77: 1404–1417.

Loew, L. M., L. B. Cohen, J. Dix, E. N. Fluhler, V. Montana, G. Salama, and J. Y. Wu. 1992. A naphthyl analog of the aminostyryl pyridinium class of potentiometric membrane dyes shows consistent sensitivity in a variety of tissue, cell, and model membrane preparations. *J. Membr. Biol.* 130:1–10.

Loew, L. M., L. B. Cohen, B. M. Salzberg, A. L. Obain, and F. Bezanilla. 1985. Charge-shift probes of membrane potential: characterization of aminostyrylpyridinium dyes on the squid giant axon. *Biophys. J.* 47: 71–77.

Loew, L. M., and L. L. Simpson. 1981. Charge-shift probes of membrane potential: A probable electrochromic mechanism for p-aminostyrylpyridinium probes on a hemispherical lipid bilayer. *Biophys. J.* 34:353–365.

London, J. A., L. B. Cohen, and Y. J. Wu. 1989. Optical recordings of the cortical response to whisker stimulation before and after addition of an epileptogenic agent. *J. Neurosci.* 9:2182–2190.

McGahren, E. D., J. M. Beach, and B. R. Duling. 1998. Capillaries demonstrate membrane potential changes in response to pharmacological stimuli. *Am. J. Physiol.* 274:H60–H65.

Montana, V., D. L. Farkas, and L. M. Loew. 1989. Dual-wavelength ratiometric fluorescence measurements of membrane potential. *Biochemistry.* 28:4536–4539.

Orbach, H. S., L. B. Cohen, and A. Grinvald. 1985. Optical mapping of electrical activity in rat somatosensory and visual cortex. *J. Neurosci.* 5:1886–1895.

Rohr, S., and B. M. Salzberg. 1994. Characterization of impulse propagation at the microscopic level across geometrically defined expansions of excitable tissue: multiple site optical recording of transmembrane voltage (MSORTV) in patterned growth heart cell cultures. *J. Gen. Physiol.* 104:287–309.

Salama, G., R. Lombardi, and J. Elson. 1987. Maps of optical action potentials and NADH fluorescence in intact working hearts. *Am. J. Physiol.* 252:H384–H394.

Zhang, J., R. M. Davidson, M. Wei, and L. M. Loew. 1998. Membrane electric properties by combined patch clamp and fluorescence ratio imaging in single neurons. *Biophys. J.* 74:48–53.